Analytical methods for azimuthal thermo-acoustic modes in annular combustion chambers

By M. Bauerheim† AND T. Poinsot‡

1. Motivations and objectives

Large power densities in gas turbines can be accompanied by combustion instabilities (Culick & Kuentzmann 2006; Lieuwen & Yang 2005) due to a coupling between the flames and acoustics, creating high pressure and heat release oscillations in the chamber. Such oscillations may destroy the whole propulsion system and combustion instabilities have been a key issue for aeronautics and propulsion systems (Candel 2002; Culick & Kuentzmann 2006; Lieuwen & Yang 2005) especially in high-performance engines (Harrje & Reardon 1972; Culick 1987) for a long time. Full-scale experiments in this field are difficult (Poinsot *et al.* 1987; Lee & Lieuwen 2003; Lee & Anderson 1999) and numerical simulations have been used heavily to replicate the complex mechanisms involved in combustion instabilities in full-scale geometries (Wolf *et al.* 2009; Staffelbach *et al.* 2009; Wolf *et al.* 2010). These simulations are not sufficient to understand or control unstable modes: low-order models and theory on simplified geometries (Dowling 1995, 1997; Kopitz *et al.* 2005; Nicoud *et al.* 2007) are needed to guide both large-eddy simulations (LES) and experiments. Annular chambers used in gas turbines sometimes exhibit a specific class of unstable modes: azimuthal modes (Figure 1) propagating along the azimuthal direction $\vec{e}_\theta$ and not only in the longitudinal direction $\vec{e}_z$ (Candel 1992; Crighton *et al.* 1992; Lieuwen & Yang 2005; O'Connor *et al.* 2015). Mechanisms leading to azimuthal instabilities are more complex than those encountered in longitudinal configurations. As presented in Figure 2, which focuses on neighboring burners of an annular rig (Figure 1, right), azimuthal modes have two effects on the flame: (1) the unsteady pressure in the chamber leads to unsteady flow rates in the burners and acts like a clock that modulates the reactant flow rate in the burners (Figure 2-a); (2) the unsteady azimuthal velocity field induces a transverse oscillation of the flames (Figure 2-b), especially in burners located at velocity antinodes (Blimbaum *et al.* 2012; O'Connor *et al.* 2015). These two mechanisms can promote flame-flame interaction (Figure 2-c, also known as flame merging), but the effect of this interaction on thermo-acoustic instabilities is not fully understood (Lespinasse *et al.* 2013; O'Connor & Lieuwen 2012). Note that the mechanisms presented in Figure 2 assume that burners are compact with respect to the acoustic wavelength, an assumption that is usually valid for azimuthal modes in annular combustors: $\lambda \simeq 2L_c \gg a$ where λ is the azimuthal wavelength of the first mode (which is usually the strongest one), $2L_c = 2\pi R_c$ is the perimeter of the annular chamber, and $a = \sqrt{4S_i/\pi}$ is the burner diameter.

The situation is more complex when the annular chamber is coupled to an annular plenum (Figure 1 right). Because they have different radii ($R_p \neq R_c$) and mean sound speeds ($c_u^0 \neq c^0$) and thus different resonant frequencies, azimuthal modes should exist

† CERFACS, Toulouse, France
‡ IMFT, CNRS, Toulouse, France

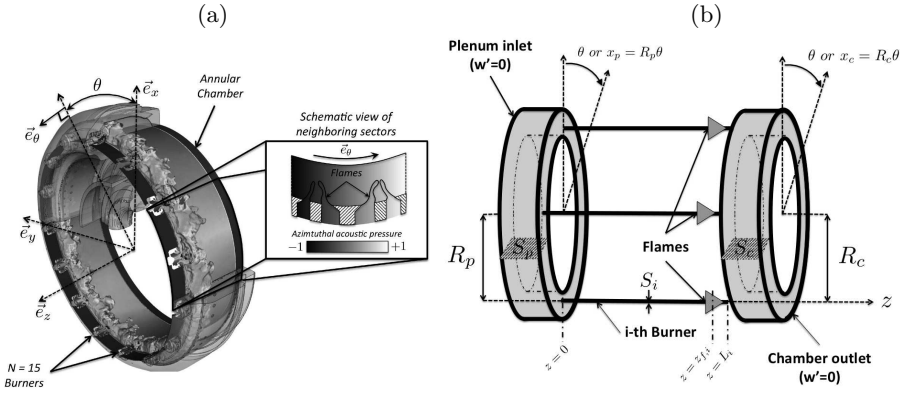

FIGURE 1. (a): Azimuthal combustion instability (pressure fluctuations along the azimuthal direction $\vec{e}_\theta$) in an annular engine and zoom on two neighboring burners. (b): annular chamber connected to N burners fed by a common annular plenum.

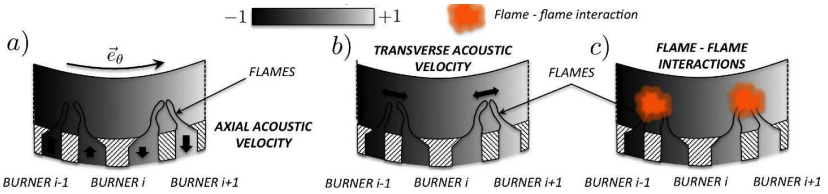

FIGURE 2. Acoustic pressure field for azimuthal combustion instabilities: the azimuthal mode acts like a clock modulating the axial mass flow rate in the burners (a) but also creates a transverse excitation (b). Both mechanisms can also generate flame-flame interaction (c).

only in one cavity (plenum or chamber) at a time: the two cavities are decoupled (Bauerheim *et al.* 2014*b*). However, experiments and simulations (Bourgouin 2014; Camporeale *et al.* 2011; Bauerheim *et al.* 2014*b*) show that azimuthal modes can develop simultaneously in both cavities. This raises questions of how annular cavities can couple and which cavity drives the azimuthal mode. This information is important in order to control azimuthal modes in industrial gas turbines, which usually contain multiple cavities.

The structure of azimuthal modes is a continuous topic of discussion. Krebs *et al.* (2002) proved that multiple modal structures coexist in a real gas turbine: spinning, standing, or even mixed modes appear successively, and instabilities can switch from one structure to another (Schuermans *et al.* 2006; Evesque *et al.* 2003). Each azimuthal mode is composed of two components, e.g. clockwise/counter-clockwise. Depending on the configuration, these two components can be "degenerate" (same frequency) or "non-degenerate" (different frequencies and stability criteria (Perrin & Charnley 1973)). The final mode structure is determined by the combination of these two components, which is still an open topic today. A first LES attempt to understand this peculiar phenomenon was carried out by Wolf *et al.* (2009), showing that swirlers induce a mean azimuthal velocity which can modify the flame-flame or flame-acoustics interactions and influence the occurrence of spinning or standing modes, as also observed in the Dawson's experiment (Worth & Dawson 2012). Schuermans et al. (2006) have also argued that at high-pressure oscillation levels, only turning modes would survive because of non-linear effects. Noiray *et al.* (2011) demonstrated that turning modes would appear only in purely axisymmetric cases, standing or mixed modes occurring otherwise. However, the effect of the modes

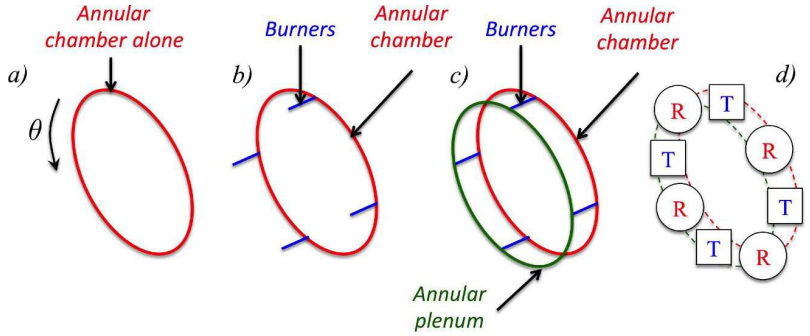

FIGURE 3. Annular configurations: a) Simple annulus, b) One annulus coupled with N burners (BC), c) Two annular cavities coupled with N burners (PBC), and d) Network representation of the annular combustor with propagation (R) and interaction (T) matrices.

structure (standing, spinning) on the flame-acoustics interactions and therefore on instabilities is still an open question. For instance, the new mode pattern ("slanted mode") observed by the EM2C group in their academic annular combustor MICCA (Bourgouin *et al.* 2015) calls for novel theoretical developments.

This paper presents recent progress in analytical methods developed for azimuthal modes using network models. Section 2 derives key parameters controlling azimuthal modes in order to classify them. It focuses mainly on coupled/decoupled modes (Section 2.1) and symmetry breaking (Section 3).

2. Key features controlling azimuthal modes stability and dynamics

Annular chambers of real gas turbines are usually characterized by numerous modes in the low frequency range (Nicoud *et al.* 2007; Camporeale *et al.* 2011): typically 10 to 30 modes can be identified in a large scale industrial combustor between 0 and 300 Hz. One interesting issue is therefore to identify them. For example, both standing and spinning (Krebs *et al.* 2002; Evesque *et al.* 2003) modes are observed in industrial configurations (Krebs *et al.* 2002; Noiray *et al.* 2011; Wolf *et al.* 2012; Schuller *et al.* 2012), but predicting which mode type will appear in practice remains difficult (Noiray *et al.* 2011; Ghirardo & Juniper 2013; Ghirardo *et al.* 2015). Other typical categories are "longitudinal vs. azimuthal modes," "normal vs. non-normal modes," or "modes involving only one part of the combustor (decoupled modes) vs. modes resonating in the whole system (coupled modes)" (Krebs *et al.* 2002; Lieuwen & Yang 2005; Camporeale *et al.* 2011; Pankiewitz & Sattelmayer 2003). Knowing that a predicted mode with a specific nature is driven only by a certain part of the combustor is obviously a key asset before applying any passive control strategy (Stow & Dowling 2003; Campa & Camporeale 2014).

2.1. *Coupled vs. decoupled modes*

The classification of modes in annular combustors is a challenging task. Even if $3D$ acoustic solvers can determine whether a mode is present in a certain part of the combustor or not, they cannot describe the basic mechanisms leading to the growth of these modes (Camporeale *et al.* 2011; Campa & Camporeale 2014). For instance, for combustion chambers including an annular plenum coupled with an annular chamber, theory is useful for understanding how azimuthal modes in the plenum and in the chamber can interact or live independently.

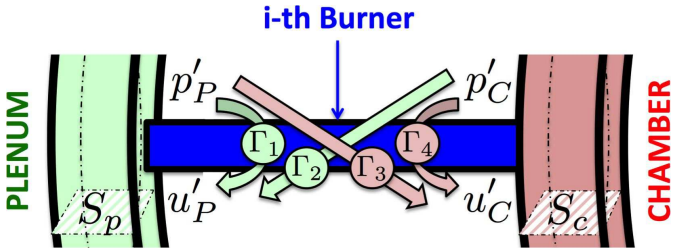

FIGURE 4. Zoom on the burner connecting the annular plenum and the annular chamber. Acoustic pressure (p') and velocity (u') in the plenum (subscript $_P$) and in the chamber (subscript $_C$) are coupled. These interactions are modeled by four coupling parameters $\Gamma_{k=1..4}$.

These issues can be studied for an annular chamber (subscript c) connected to N burners fed by a common annular plenum (subscript p), called a plenum-burner-chamber (PBC) configuration (c in Figure 3), using a network model (Bauerheim *et al.* 2014*b*). The period of the first azimuthal mode of the chamber without flames is $\tau_c^0 = 2L_c/c^0$, and its frequency is $f_c^0 = c^0/2L_c$. For $N = 1$, the dispersion relation becomes

$$\begin{aligned}(\Gamma_1\Gamma_4 - \Gamma_2\Gamma_3)\sin(2kL_c)\sin(2k_uL_p) + 2\Gamma_1[1-\cos(2kL_c)]\sin(2k_uL_p)\\ +2\Gamma_4[1-\cos(2k_uL_p)]\sin(2kL_c) + 4[1-\cos(2kL_c)][1-\cos(2k_uL_p)] = 0,\end{aligned} \tag{2.1}$$

where $k = \omega/c^0$ and $k_u = \omega/c_u^0$. c^0 and c_u^0 are the sound speeds in the burnt/unburnt gases (Figure 1). As shown in Figure 4, the acoustic velocities u' in the plenum and in the chamber are coupled to the acoustic pressure in the burner and the flame: for instance $u'_P = \Gamma_1 p'_P + \Gamma_2 p'_C$. These interactions involve four coupling parameters:

$$\Gamma_1 = -\frac{S_i}{2S_p}\text{cotan}(k_uL_i) \quad \Gamma_2 = \frac{S_i}{2S_p}\frac{1}{\sin(k_uL_i)} \quad \Gamma_3 = \frac{S_i\rho^0c^0}{2S_c\rho_u^0c_u^0}\frac{1+n^{j\omega\tau}}{\sin(k_uL_i)} \tag{2.2}$$

$$\Gamma_4 = -\frac{S_i\rho^0c^0}{2S_c\rho_u^0c_u^0}(1+n^{j\omega\tau})\text{cotan}(k_uL_i). \tag{2.3}$$

Γ_1 is the coupling parameter associated with the plenum/burner junction, and Γ_4 with the chamber/burner junction. Γ_2 and Γ_3 control the interaction between the two annular cavities. Only the coupling parameters of the chamber (Γ_3 and Γ_4) depend on the $n-\tau$ flame model. This case corresponds to a pressure coupling: for example, if the azimuthal mode imposes a pressure node in the chamber (i.e. $p'_c = 0$), then the interactions $\Gamma_2 p'_C$ and $\Gamma_4 p'_C$ are null, independently of the coupling parameter values. This simple case allows the identification of three situations, for which the conclusion still holds for larger numbers of burners:

- Fully decoupled (FD) modes: when all coupling parameters Γ_i are null, solutions of Eq. (2.1) of order m are $f_c^0 = mc^0/2L_c$ (pure azimuthal decoupled mode in the chamber) or $f_p^0 = mc_u^0/2L_p$ (pure azimuthal decoupled mode in the plenum).
- Weakly coupled (WC) modes (a in Figure 5): when coupling factors are not null but satisfy $\|\Gamma_{k=1..4,i}\| \ll 1$, solutions are close to the FD modes and can be searched as $f_c = f_c^0 + \delta f$ and $f_p = f_p^0 + \delta f$. A Taylor expansion of the dispersion relation yields the solutions in the case where the two annular cavities are not naturally coupled, i.e. when f_p^0 and f_c^0 are not multiples of each other

$$f_c = \frac{mc^0}{2L_c} - \frac{c^0\Gamma_4^0}{4\pi L_c} \text{ and } f_p = \frac{mc_u^0}{2L_p} - \frac{c_u^0\Gamma_1^0}{4\pi L_p}. \tag{2.4}$$

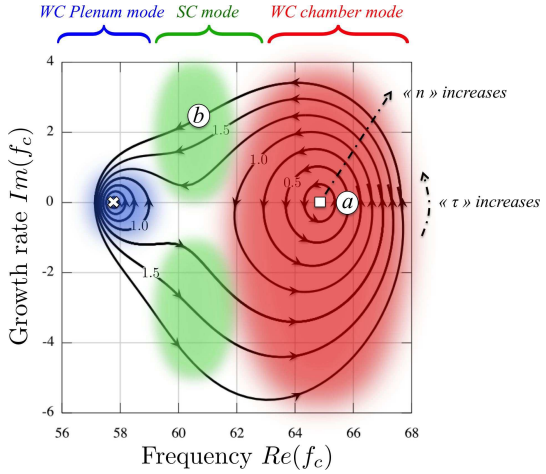

FIGURE 5. Stability map $\{Re(f_c), Im(f_c)\}$ of a PBC configuration with $N = 4$ burners where the FTF parameters are varied: n from 0.25 to 1.75 and τ/τ_c^0 from 0 to 1.0, showing the bifurcation between WC and SC modes at $n = 1.25$. FD modes: crosses (plenum) and squares (chamber). Shading emphasizes mode type.

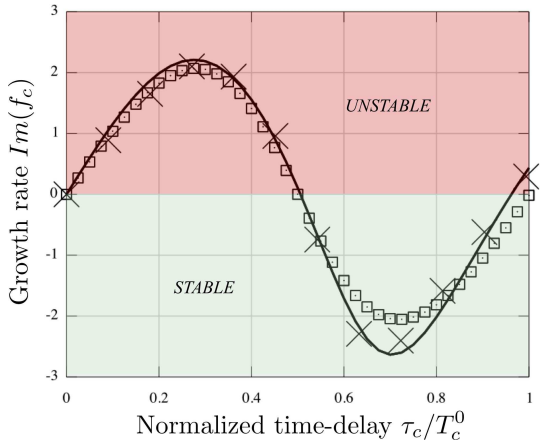

FIGURE 6. Growth rate $Im(f_c)$ of the first chamber mode ($m = 1$) in a PBC combustor with $N = 4$ burners where $n = 1.57$. The time-delay varies from 0 to τ_c^0, where $\tau_c^0 = 1/f_c^0$. $Im(f_c)$ is estimated by the full analytical formula $f_c = \frac{c^0}{2L_c} + \frac{c^0 N \Gamma_4^0}{4\pi L_c}$ (squares), a semi-analytical resolution (solid line) of the dispersion relation and a $3D$ Helmholtz solver ($\times$).

The f_p and f_c modes correspond to "plenum" (WC plenum modes in Figure 5, left) or "chamber" (WC chamber modes in Figure 5, right) modes. This result obtained for $N = 1$ burner has been extended to configurations with N burners as follows (Bauerheim *et al.* 2014*b*,*a*): for the WC chamber mode, the frequency scales like $f_c = \frac{mc^0}{2L_c} - \frac{c^0 N \Gamma_4^0}{4\pi L_c}$. Γ_4^0 is the evaluation of the coupling parameter Γ_4 at the frequency of the corresponding FD mode, i.e. $f = f_c^0$. The flame delay τ is normalized by the period of the first azimuthal mode τ_p^0 or τ_c^0. This analytical expression is validated against a semi-analytical method as well as a 3D Helmholtz solution in Figure 6.

- Strongly coupled (SC) modes (b in Figure 5): When the WC assumption $\|\Gamma_{k=1..4,i}\| \ll 1$ is not satisfied, the two annular cavities can couple and oscillate at a frequency that is

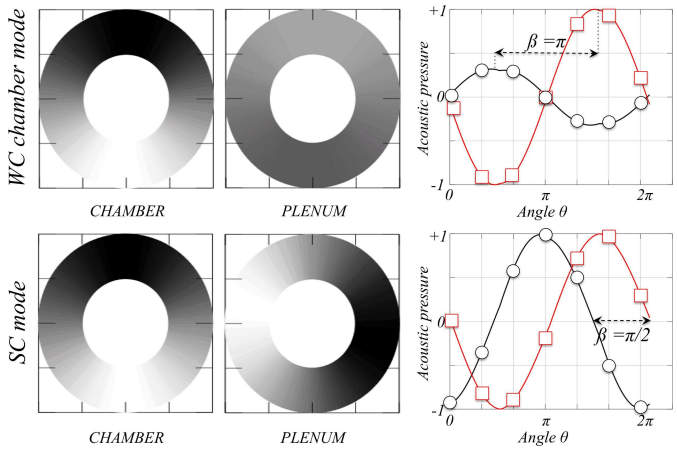

FIGURE 7. Mode structure for $N = 4$ burners in the chamber (left and squares) and in the plenum (middle and circles) for a WC chamber mode (top row: $n = 0.5$; $\tau/\tau_c^0 = 0$) and SC mode (bottom row: $n = 1.75$; $\tau/\tau_c^0 = 0.5$).

not close to f_p^0 or f_p^0. In this case, the acoustic mode cannot be identified as "plenum" or "chamber" mode since the whole combustor resonates: a bifurcation occurs (SC modes in Figure 5, middle) known as a veering effect (Mace & Manconi 2012). Only partially analytical solutions can be obtained in such a situation. In particular, SC modes in Figure 5 are obtained by solving the dispersion relation numerically.

This analytical study (Bauerheim *et al.* 2014*b*) allows the classification of azimuthal modes as FC, WC and SC modes. For the first two categories, the acoustic mode is present in only one annular cavity and can be identified as "plenum" or "chamber" mode (Figure 7, top). However, when the flames tune one annular cavity so that it matches the resonant frequency of the second cavity, a bifurcation in the stability map occurs: here, the mode cannot be classified as "plenum" or "chamber" modes since the whole combustor resonates (Figure 7, bottom). A phase-lag β, controlled by the time-delay τ, between the annular chamber and the plenum is observed in Figure 7 for both WC and SC regimes. In the WC case, $\tau/\tau_c^0 = 0$ leads to a phase-lag $\beta = \pi$, whereas in the SC case, $\tau/\tau_c^0 = 0.5$ yields a phase-lag $\beta = \pi/2$. Bourgouin *et al.* (2014) have investigated this phenomenon analytically on the MICCA annular experiment. They found that for a WC plenum mode, τ/τ_c^0 leads to $\beta = 0$ (or π if $Re(f_c) > Re(f_c^0)$ as in Figure 7) and then decreases with the time-delay. For SC modes, network models show that the maximum coupling is obtained when $\beta = \pi/2$ for this $N = 4$ burner configuration (Bauerheim *et al.* 2014*b*).

3. Degenerate modes and symmetry breaking

A specificity of azimuthal modes is degeneracy: an acoustic mode in a simple annular chamber can turn clockwise or counter-clockwise, leading to two possible modes for each eigenfrequency. Understanding when and how azimuthal modes are degenerate brings up many other issues such as symmetry breaking which are discussed below.

3.1. *Mixing different burner types*

Frequencies and stability maps obtained in Section 2.1 have been validated against $3D$ acoustic simulations in many applications, from academic combustors (Bauerheim *et al.*

2014*b*,*a*) to industrial gas turbines (Parmentier *et al.* 2012; Bauerheim *et al.* 2015). However, only axisymmetric combustors were investigated. Recently, the need for considering non-symmetric combustors has been considered, mainly for investigating novel passive techniques to control azimuthal modes. For instance, introducing Helmholtz resonators (Stow & Dowling 2003; Campa & Camporeale 2014), baffles (Dawson & Worth 2014), or different types of burners (Berenbrink & Hoffmann 2001; Moeck *et al.* 2010) may damp unstable modes but may also break the rotational symmetry of the configuration. For the latter option, choosing which burner types must be mixed in a chamber and how to distribute them along the azimuthal direction to damp modes is an open topic that analytical studies can help clarify.

Network models applied to a burner-chamber (BC) configuration (b in Figure 3) can be used to extend the results of Section 2.1 to non-symmetric combustors containing an arbitrary number of burners N (Bauerheim *et al.* 2014*a*). Burners can differ from each other because of their geometric characteristics, which may lead to different FTFs for each flame. This yields different coupling parameters $\Gamma_{4,i}$ (in a BC configuration, only one type of coupling parameter exists, so that subscript 4 can be omitted). For WC modes, the frequencies of the azimuthal mode of order m are

$$f_m^{\pm} = \frac{mc^0}{2L_c} - \frac{c^0}{4\pi L_c}(\Sigma_0 \pm \mathcal{S}_0) \tag{3.1}$$

where

$$\Sigma_0 = \sum_{i=1}^{N} \Gamma_i^0 \quad \text{and} \quad \mathcal{S}_0 = \sqrt{\sum_{i,j=1}^{N} \Gamma_i^0 \Gamma_j^0 \cos\left(\frac{4m\pi}{N}(j-i)\right)}. \tag{3.2}$$

This result demonstrates that the stability of non-symmetric annular combustors is controlled by two parameters: (1) the "coupling strength" Σ_0, which is the sum of all coupling parameters of the system and is independent of the pattern used to distribute the burners in the chamber. It corresponds to a symmetric effect associated to a "mean flame" FTF. For instance, in a case with $N = 24$ burners with two types of burners, characterized by a coupling parameter Γ_A^0 (4 flames) and Γ_B^0 (20 flames), the coupling parameter is $\Sigma_0 = 4\Gamma_A^0 + 20\Gamma_B^0$. Thus, it is equivalent to using 24 identical burners with a coupling parameter $\Gamma^0 = \frac{4}{24}\Gamma_A^0 + \frac{20}{24}\Gamma_B^0$. Consequently, this parameter can be changed, for example by using 8 burners of type A and 16 of type B, to stabilize one or multiple azimuthal modes (Figure 8) (Bauerheim *et al.* 2014*a*). (2) the "splitting strength" $\mathcal{S}_0$ is the quantity that "splits" the two azimuthal mode frequencies f_m^+ and f_m^- (sign $\pm$ in Eq. (3.2)). A convenient form for $\mathcal{S}_0$ is obtained by using the spatial Fourier transform of the coupling parameter distribution γ

$$\mathcal{S}_0 = \sqrt{\gamma(2m)\gamma(-2m)}, \text{ where } \gamma(k) = \sum_{i=1}^{N} \Gamma_i^0 e^{-\frac{j2k\pi i}{N}}. \tag{3.3}$$

It shows that only specific patterns can affect the azimuthal mode stability. They correspond to the $\pm 2m^{th}$ Fourier coefficient γ of the coupling parameter or heat-release distribution. Therefore, unlike the coupling strength Σ_0, this parameter can be changed by modifying the pattern of the burner types along the annular chamber.

Note that since the splitting strength damps one mode but always increases the growth rate of the second one by $Im(\mathcal{S}_0)/2$, using a non-zero splitting strength always makes the system less stable (Figure 8): according to theory, combining different burners is not a solution to control one mode. However, mixing different burner types can become

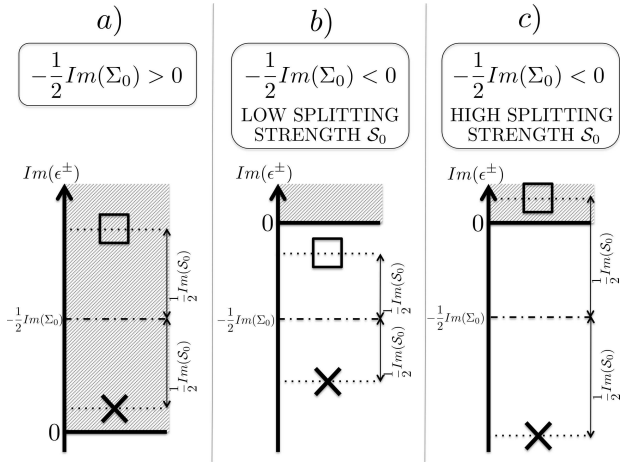

FIGURE 8. Three stability cases given by the normalized growth rate $Im(\epsilon^{\pm}) = \frac{2\pi L_c}{c^0} Im(f^{\pm})$ of the two components (X and squares) depending on the coupling strength Σ_0 and splitting strength $\mathcal{S}_0$. (a) The coupling strength leads to an unstable mode. (b) The coupling strength leads to a stable mode since the splitting strength is low. (c) The coupling strength should lead to a stable mode, but because of a high splitting strength, one of its component is unstable.

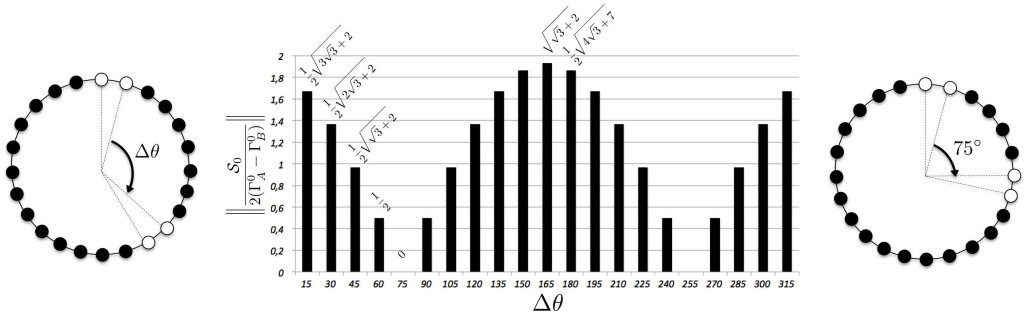

FIGURE 9. The reduced splitting strength $\mathcal{K}$ for several patterns where two burners of type A are kept together at the same place and two others are changed azimuthally so that only one parameter controls the burner distribution: the angle $\Delta\theta$. Optimal patterns are found analytically to reduce the splitting strength, for example using $\Delta\theta = 75^{\circ}$ yields $\mathcal{K} = 0$ (right).

useful to modify Σ_0 in order to control multiple modes, or one acoustic mode at different operating points. In this case, the burners can be rearranged along the annular chamber to reduce the splitting strength. For instance, when only two burner types are used, the splitting strength reduces to

$$\|\mathcal{S}_0\| = 2\mathcal{K} \left\| \Gamma_A^0 - \Gamma_B^0 \right\|, \tag{3.4}$$

where $\mathcal{K}$ is a constant that only depends on the pattern (Bauerheim *et al.* 2014*a*) whereas $\Gamma_A^0 - \Gamma_B^0$ depends only on the response difference between the two burner types.

Equation (3.4) shows that the splitting strength increases when the difference between the two burner types $\|\Gamma_A^0 - \Gamma_B^0\|$ increases, which is necessary to control modes by changing significantly Σ_0. But it also reveals that the splitting strength can be reduced by changing the pattern, i.e. $\mathcal{K}$: an optimization procedure over all patterns possible can be performed to find the pattern that minimizes $\mathcal{K}$, in order to suppress this side-effect due to splitting. Determining all patterns that lead to $\mathcal{K} = 0$ is a complicated mathe-

matical exercise in general. For example, in a 24 burner machine, where 4 "different" (Type 2, white in Figure 9) burners are inserted in the annulus (Berenbrink & Hoffmann 2001) as two pairs of burners separated by an angle $\Delta\theta$, analytical results show that specific rearrangements of burners can lead to $\mathcal{K} = 0$, and therefore a zero splitting effect (Figure 9, when $\Delta\theta = 75°$ or $\Delta\theta = 225°$) (Bauerheim *et al.* 2014*a*). Again, such an optimization procedure is made possible only because of recent progress in theoretical tools for thermo-acoustics, since computing all patterns with a $3D$ Helmholtz solver is not feasible yet (more than 2000 patterns exist for a 24 burner configuration with $N_A = 4$ burners of type A, and more than $77,000$ for $N_A = 6$.).

3.2. *Breaking symmetry to control azimuthal modes*

For annular combustors, splitting can be introduced on purpose or be a consequence of undesired differences in burners due to manufacturing tolerances. When splitting is introduced on purpose by the engine designers, the objective is usually to damp unstable modes: symmetry breaking is created by mixing different burner types (Section 3.1) which is called Geometrical Symmetry (GS) breaking (Bauerheim *et al.* 2014*b*). Other types of symmetry breaking can be investigated to highlight their effect on azimuthal mode stability. For instance, the introduction of a mean swirl motion, called Flow Symmetry (FS) breaking, has been investigated recently (Bauerheim *et al.* 2014*b*). It shows that an additional splitting effect due to the mean flow is present and can interact non-linearly with the splitting due to the GS breaking $\mathcal{S}_0$

$$\mathcal{S}_M = \sqrt{\mathcal{S}_0^2 + 4\pi^2 M_\theta^2} \tag{3.5}$$

where $\mathcal{S}_M$ is the total splitting strength and M_θ is the mean azimuthal Mach number. The anaytical solution of the dispersion equation allows to analyse three typical situations:

- GS breaking: When $\|\mathcal{S}_0\| >> 2\pi M_\theta$, the splitting is mainly affected by the difference between burners, ie by GS breaking. When $Im(\mathcal{S}_0) \neq 0$, splitting always makes the mode less stable, as mentioned by Davey & Salwen (1994) for hydrodynamic modes. Note that this conclusion may differ for SC modes (Salas 2013).
- FS breaking: If $\|\mathcal{S}_0\| << 2\pi M_\theta$, the symmetry breaking is driven by the flow itself. However, since M_θ is real, the resulting splitting strength has a null imaginary part: the mode is non-degenerate but the stability is unchanged.
- FS+GS breaking: When both $\mathcal{S}_0$ and M_θ are significant, the two splitting effects (FS and GS) interact non-linearly (the resulting splitting strength is not just the sum of $\mathcal{S}_0$ and $2\pi M_\theta$): FS breaking can increase or decrease the splitting effect and affect the stability of the configuration.

This result suggests that symmetry breaking is an important element of control strategies for azimuthal modes (using, for example, baffles or Helmholtz resonators to damp acoustic modes). Other engine modifications can also produce symmetry breaking: introducing additional effusive plates will induce a mean swirl and a FS breaking effect; adding spark plugs or ignition injectors will introduce GS breaking. Even if thermo-acoustics was not the reason for these modifications, it will be affected by these changes.

4. Conclusion

Mechanisms leading to azimuthal instabilities in annular chambers have been investigated using theoretical methods based on one-dimensional acoustic networks and flame transfer functions. These theoretical tools are mandatory to understand experimental

and LES results as they provide direct insight into the effects of symmetry breaking and the structure of modes appearing in these chambers.

5. Acknowledgements

The support of the ERC project 319067-INTECOCIS (Introducing Exascale Computing in Combustion Instabilities Simulations) is gratefully acknowledged.

REFERENCES

Bauerheim, M., Ndiaye, A., Constantine, P., Iaccarino, G., Moreau, S. & Nicoud, F. 2014*a* Uncertainty quantification of thermo-acoustic instabilities in annular combustors. *Proceedings of the Summer Program,* Center for Turbulence Research, Stanford University, pp. 209–210.

Bauerheim, M., Nicoud, F. & Poinsot, T. 2015 Theoretical analysis of the mass balance equation through a flame at zero and non-zero mach numbers. *Combust. Flame* **162** (1), 60 – 67.

Bauerheim, M., Parmentier, J.-F., Salas, P., Nicoud, F. & Poinsot, T. 2014*b* An analytical model for azimuthal thermo-acoustic modes in an annular chamber fed by an annular plenum. *Combust. Flame* **161** (5), 1374 – 1389.

Berenbrink, P. & Hoffmann, S. 2001 Suppression of dynamic combustion instabilities by passive and active means. In *ASME Turbo Expo 2001. Paper 2001-GT-42*.

Blimbaum, J., Zanchetta, M., Akin, T., Acharya, V., O'Connor, J., Noble, D. & Lieuwen, T. 2012 Transverse to longitudinal acoustic coupling processes in annular combustion chambers. *Int. J. Spray Combust. Dyn.* **4** (4), 275–298.

Bourgouin, J.-F. 2014 Dynamique de flamme dans les foyeres annulaires comportant des injecteurs multiples. PhD thesis, Ecole Centrale de Paris (EM2C).

Bourgouin, J.-F., Durox, D., Moeck, J., Schuller, T. & Candel, S. 2014 Characterization and modeling of a spinning thermo-acoustic instability in an annular combustor equipped with multiple matrix injectors. *ASME Paper 2014-GT-25067*.

Bourgouin, J. F., Durox, D., Moeck, J. P., Schuller, T. & Candel, S. 2015 A new pattern of instability observed in an annular combustor: The slanted mode. *Proc. Combust. Inst.* **35** (3), 3237–3244.

Campa, G. & Camporeale, S. 2014 Influence of nonlinear effects on the limit cycle in a combustion chamber equipped with helmholtz resonators. *ASME Paper 2014-GT-25228*.

Camporeale, S., Fortunato, B. & Campa, G. 2011 A finite element method for three-dimensional analysis of thermo-acoustic combustion instability. *J. Eng. Gas Turbines Power* **133** (1).

Candel, S. 1992 Combustion instabilities coupled by pressure waves and their active control. In *24th Symp. (Int.) on Combustion*, pp. 1277–1296. The Combustion Institute, Pittsburgh.

Candel, S. 2002 Combustion dynamics and control: progress and challenges. *Proc. Combust. Inst.* **29** (1), 1–28.

Crighton, D. G., Dowling, A. P., Williams, J. E. F., Heckl, M. & Leppington, F. 1992 *Modern methods in analytical acoustics*. New York: Springer Verlag.

Culick, F. E. C. 1987 Combustion instabilities in liquid-fueled propulsion systems - an overview. In *AGARD 72B PEP meeting*.

Culick, F. E. C. & Kuentzmann, P. 2006 *Unsteady Motions in Combustion Chambers for Propulsion Systems*. NATO Research and Technology Organization.

Davey, A. & Salwen, H. 1994 On the stability in an elliptic pipe which is nearly circular. *J. Fluid Mech.* **281**, 357–369.

Dawson, J. & Worth, N. 2014 The effect of baffles on self-excited azimuthal modes in an annular combustor. *Proc. Combust. Inst.* **35**, 3283–3290.

Dowling, A. P. 1995 The calculation of thermo-acoustic oscillations. *J. Sound Vib.* **180** (4), 557–581.

Dowling, A. P. 1997 Nonlinear self-excited oscillations of a ducted flame. *J. Fluid Mech.* **346**, 271–290.

Evesque, S., Polifke, W. & Pankiewitz, C. 2003 Spinning and azimuthally standing acoustic modes in annular combustors. In *9th AIAA/CEAS Aeroacoustics Conference*, AIAA Paper 2003-3182.

Ghirardo, G. & Juniper, M. 2013 Azimuthal instabilities in annular combustors: standing and spinning modes. *Proc. R. Soc. Lond. A*, 2013-0232.

Ghirardo, G., Juniper, M. & Moeck, J. 2015 Stability criteria for standing and spinning waves in annular combustors. *ASME Paper GT2015-43127*.

Harrje, D. J. & Reardon, F. H. 1972 Liquid propellant rocket instability. *Tech. Rep.* Report SP-194. NASA.

Kopitz, J., Huber, A., Sattelmayer, T. & Polifke, W. 2005 Thermoacoustic stability analysis of an annular combustion chamber with acoustic low order modeling and validation against experiment. In *Int'l Gas Turbine and Aeroengine Congress & Exposition*. Reno, NV.

Krebs, W., Flohr, P., Prade, B. & Hoffmann, S. 2002 Thermoacoustic stability chart for high intense gas turbine combustion systems. *Combust. Sci. Tech.* **174**, 99–128.

Lee, D. & Lieuwen, T. 2003 Premixed flame kinematics in a longitudinal acoustic field. *J. Prop. Power* **19** (5), 837–846.

Lee, D. S. & Anderson, T. J. 1999 Measurements of fuel/air-acoustic coupling in lean premixed combustion systems. In *37th AIAA Aerospace Sciences Meeting and Exhibit* (ed. A. P. 99-0450). Reno, NV.

Lespinasse, F., Baillot, F. & Boushaki, T. 2013 Responses of V-flames placed in an HF transverse acoustic field from a velocity to pressure antinode. *C. R. Acad. Sci. Mecanique* **341** (1-2), 110–120.

Lieuwen, T. & Yang, V. 2005 *Combustion Instabilities in Gas Turbine Engines. Operational Experience, Fundamental Mechanisms and Modeling*. Prog. in Astronautics and Aeronautics , Vol 210.

Mace, B. & Manconi, E. 2012 Wave motion and dispersion phenomena: veering, locking, and strong coupling effects. *J. Acous. Soc. Am.* **131 (2)**.

Moeck, J., Paul, M. & Paschereit, C. 2010 Thermoacoustic instabilities in an annular flat Rijke tube. In *ASME Turbo Expo 2010 GT2010-23577*.

Nicoud, F., Benoit, L., Sensiau, C. & Poinsot, T. 2007 Acoustic modes in combustors with complex impedances and multidimensional active flames. *AIAA J.* **45**, 426–441.

Noiray, N., Bothien, M. & Schuermans, B. 2011 Investigation of azimuthal staging concepts in annular gas turbines. *Combust. Theory Model.* pp. 585–606.

O'Connor, J., Acharya, V. & Lieuwen, T. 2015 Transverse combustion instabilities: acoustic, fluid mechanic, and flame processes. *Prog. Energy Comb. Sci.* **49** (C), 1–39.

O'Connor, J. & Lieuwen, T. 2012 Recirculation zone dynamics of a transversely excited swirl flow and flame. *Phys. Fluids* **24** (075107).

Pankiewitz, C. & Sattelmayer, T. 2003 Time domain simulation of combustion instabilities in annular combustors. *J. Eng. Gas Turbines Power* **125** (3), 677–685.

Parmentier, J.-F., Salas, P., Wolf, P., Staffelbach, G., Nicoud, F. & Poinsot, T. 2012 A simple analytical model to study and control azimuthal instabilities in annular combustion chambers. *Combust. Flame* **159** (7), 2374–2387.

Perrin, R. & Charnley, T. 1973 Group theory and the bell. *J. Sound Vib.* **31** (4), 411–418.

Poinsot, T., Trouvé, A., Veynante, D., Candel, S. & Esposito, E. 1987 Vortex driven acoustically coupled combustion instabilities. *J. Fluid Mech.* **177**, 265–292.

Poinsot, T. & Veynante, D. 2011 *Theoretical and Numerical Combustion*. Third Edition (www.cerfacs.fr/elearning).

Salas, P. 2013 Aspects numériques et physiques des instabilités de combustion dans les chambres de combustion annulaires. PhD thesis, Université Bordeaux - INRIA.

Schuermans, B., Paschereit, C. & Monkewitz, P. 2006 Non-linear combustion instabilities in annular gas-turbine combustors. AIAA Paper 2006-0549.

Schuller, T., Durox, D., Palies, P. & Candel, S. 2012 Acoustic decoupling of longitudinal modes in generic combustion systems. *Combust. Flame* **159**, 1921–1931.

Staffelbach, G., Gicquel, L., Boudier, G. & Poinsot, T. 2009 Large eddy simulation of self-excited azimuthal modes in annular combustors. *Proc. Combust. Inst.* **32**, 2909–2916.

Stow, S. R. & Dowling, A. P. 2003 Modelling of circumferential modal coupling due to helmholtz resonators. In *ASME Paper 2003-GT-38168*. Atlanta, Georgia.

Wolf, P., Staffelbach, G., Balakrishnan, R., Roux, A. & Poinsot, T. 2010 Azimuthal instabilities in annular combustion chambers. *Proceedings of the Summer Program,* Center for Turbulence Research, Stanford University, pp. 259–269.

Wolf, P., Staffelbach, G., Gicquel, L., Muller, J.-D. & Poinsot, T. 2012 Acoustic and large eddy simulation studies of azimuthal modes in annular combustion chambers. *Combust. Flame* **159** (11), 3398–3413.

Wolf, P., Staffelbach, G., Roux, A., Gicquel, L., Poinsot, T. & Moureau, V. 2009 Massively parallel LES of azimuthal thermo-acoustic instabilities in annular gas turbines. *C. R. Acad. Sci. Mécanique* **337** (6-7), 385–394.

Worth, N. & Dawson, J. 2012 Self-excited circumferential instabilities in a model annular gas turbine combustor: Global flame dynamics. *Proc. Combust. Inst.* **34**, 1–8.